

# A THREE-AXIS PIEZORESISTIVE MICROMACHINED FORCE SENSOR FOR STUDYING COCKROACH BIOMECHANICS

**Michael S. Bartsch**

Mechanical Engineering, Stanford University

**Aaron Partridge**

Electrical Engineering, Stanford University

**Beth L. Pruitt**

Mechanical Engineering, Stanford University

**Robert J. Full**

Integrative Biology, University of California, Berkeley

**Thomas W. Kenny**

Mechanical Engineering, Stanford University  
Stanford, CA 94305

Email: [mbartsch@stanford.edu](mailto:mbartsch@stanford.edu)

Phone: (650)723-2279

## ABSTRACT

A millimeter-scale silicon micromachined force sensor has been designed to measure in three axes the ground reaction forces produced by the cockroach *Blaberus Discoidalis* during typical running locomotion. Each sensor consists of a large-area (5mm x 5mm) rigid plate supported at its corners by thin flexures instrumented with two ion-implanted piezoresistors each. Comparison of piezoresistive measurements among these eight strain gauges allows the applied force to be resolved into three orthogonal components. Un-amplified sensitivity to normal forces of 1.2V/N has been demonstrated with estimated normal force resolution of 7.3 $\mu$ N on an 800Hz measurement bandwidth.

## INTRODUCTION

In recent years, the South American death-head cockroach, *Blaberus Discoidalis*, has become popular as a prototype for numerous biomimetic or "life-mimicking" robot designs [1,2,3]. Of particular interest to robot designers is the seemingly erratic but highly functional running style employed by such insects. This sprawl-postured alternating tripod gait is believed to work in conjunction with the structural mechanics of muscle and exoskeleton to enable rapid locomotion which is both dynamically stable and robust, even as the cockroach traverses difficult terrain [4]. Researchers in the lab of R.J. Full have sought to quantify how various features of cockroach motion

contribute to this self-stabilization [5], primarily by measuring the ground-reaction force components produced by the cockroach as it runs over an instrumented force plate [6].

One significant lesson from these studies is that unlike animals with upright gaits, a sprawl-postured cockroach exerts sizable in-plane forces (parallel to the running surface) both laterally and in the direction of motion as it runs. These forces are typically on the order of one-third to one-half as large as the normal forces associated with running. In the direction of motion, forces exerted by the forelegs of the insect actually tend to oppose forward motion while the hind legs provide most forward thrust. Each leg of the insect also exerts lateral forces directed away from the center of the body during at least a portion of the motion of each step. These in-plane forces are believed to be crucial to the characteristically robust and dynamically self-stabilizing locomotion of the cockroach, and are therefore of great interest to robot designers.

This work presents a custom silicon micromachined three-axis force sensor designed to improve upon the ground-reaction force measurement methods currently available to the R.J. Full lab. Toward this end, the design must be able to resolve forces smaller than 0.5mN. To accurately reproduce high-frequency components of the forces exerted by the insects during running, the sensor must have a mechanical bandwidth greater than 650Hz, the natural frequency of the force plate currently used in the R.J. Full lab. Sensors must be robust enough to withstand

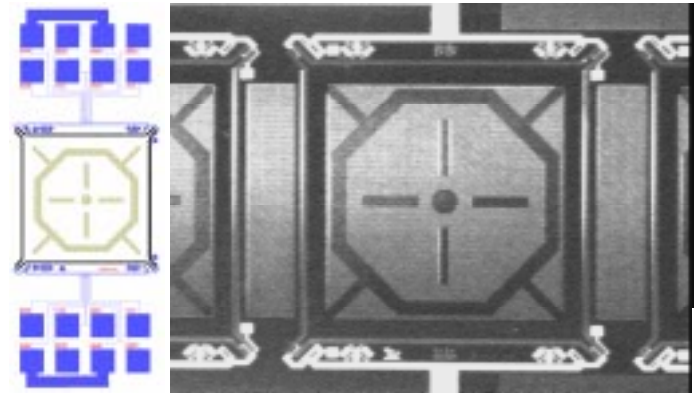
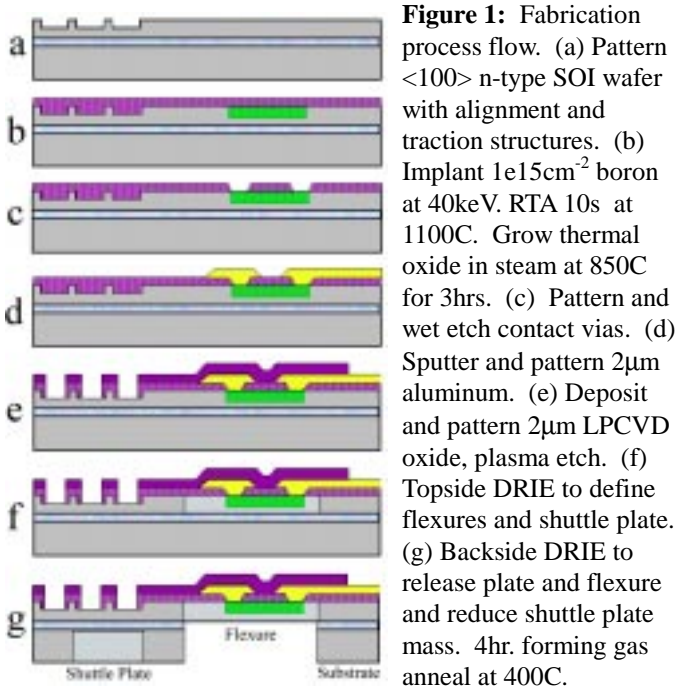


**Figure 2:** Test sensor schematic and array sensor photomicrograph. The schematic shows the configuration of a single test sensor element with oversized wire bond pads. The micrograph shows the spacing of sensor elements within one of the linear arrays. White regions correspond to aluminum interconnects. Striations on and between the shuttle plates indicate the presence of traction structures.

forces as large as 0.4N (ten times the weight of the cockroach). Such forces are produced when the insects flip over to right themselves. At the same time, the devices must be sensitive enough to accurately capture typical cockroach ground reaction forces in the range of 0-15mN. Finally, this design will also serve as a prototype for sensors enabling the study of insects much smaller than *B. Discoidalis* which have historically been beyond the capability of conventional macro-scale measurement techniques.

## DESIGN AND FABRICATION

Each single-crystal silicon sensor element consists of a rigid square plate supported at each corner by a thin, flexible beam. This design is an adaptation of a small-scale three-axis tactile sensor geometry presented by Kane [7]. The seven-mask fabrication process flow for these devices is outlined in Figure 1. The shuttle plate and flexures are defined by plasma deep reactive ion etching (DRIE) from both sides of a silicon on insulator (SOI) wafer with the buried oxide layer serving as a plasma etch stop.

The central shuttle plate measures 5mm on a side and is of full wafer thickness ( $\sim 500\text{-}600\mu\text{m}$ ). Figure 2 shows the layout of the sensor with the large shuttle plate dwarfing the flexures at each corner. The top surface of the shuttle plate is patterned with a dense array of silicon and oxide pillar structures  $4\mu\text{m}$  tall and  $15\mu\text{m}$  square. These structures, visible in Figures 2 and 3, are designed to provide traction for insects running on what would otherwise be an atomically flat silicon surface. To reduce the mass of the shuttle plate and increase its resonant frequency, large  $840\mu\text{m}$  square holes are plasma-etched into the backside of each plate, again using the buried oxide as an etch

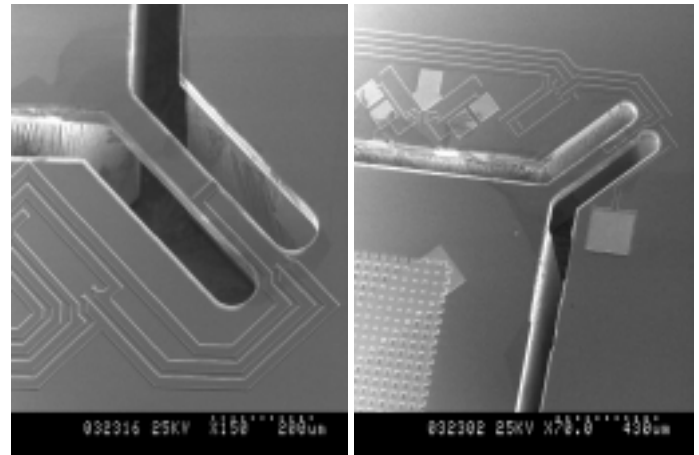


**Figure 3:** Flexure geometry. Note traction structures visible in the lower left corner of the second micrograph.

stop. The resulting structure has a predicted mechanical bandwidth of approximately 4kHz.

The shuttle plate is supported at its corners by four flexures measuring  $500\mu\text{m}$  long,  $70\mu\text{m}$  wide, and  $50\text{-}100\mu\text{m}$  thick as shown in Figure 3. To a large extent, flexure geometry ultimately dictates the specifics of sensor performance. Treating the flexures as simple fixed-guided beams, structural stiffness in the normal (out of plane) direction scales directly as the cube of the flexure thickness and inversely as the cube of flexure length. Similarly, in-plane compliance of the flexure with respect to bending scales as the cube of the flexure width divided by the cube of flexure length. Sensitivity to applied force is in turn inversely related to mechanical stiffness.

Each flexure is fabricated with two boron-doped ion-implanted piezoresistors  $200\mu\text{m}$  long and  $3\mu\text{m}$  wide, located between the substrate end of the flexure and its midpoint. One of these piezoresistive strain gauges is situated along the flexure

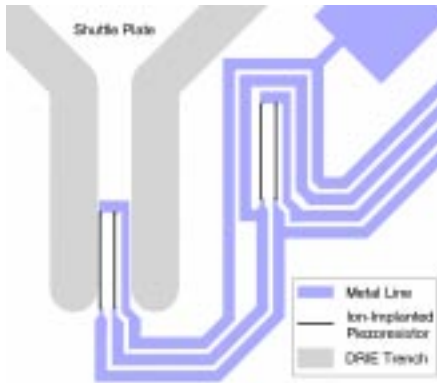


**Figure 4:** Piezo-resistor layout. Each flexure has one piezoresistor along its edge and one along its centerline. Passive legs of the Edge and Mid-flexure half-bridges can be seen to the left of the flexure.

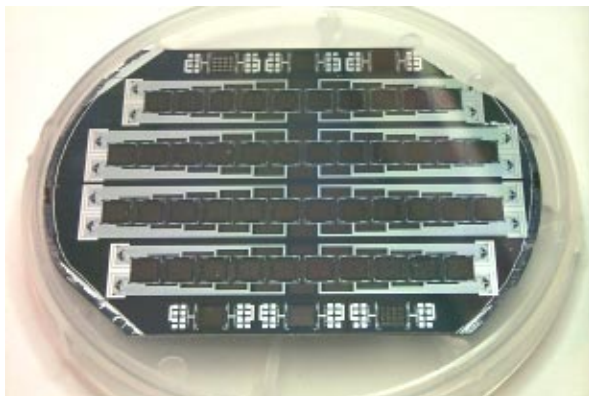


**Figure 5:** Layout of a typical 10cm device wafer. Four large sensor arrays occupy the middle of this partially diced wafer.

edge and the other is aligned with the centerline of the beam as shown in Figure 4. When the central shuttle plate deflects due to a symmetrical normal loading, both edge and midline piezoresistors experience identical strains due to pure out-of-plane bending. Under loading conditions which produce in-plane deflection, bending of the flexure will subject the flexure-edge piezoresistor to significant strains. The mid-flexure strain gauge, however, will experience negligible net average strain as its location coincides with the neutral axis of the flexure with respect to in-plane bending. Piezoresistive sensitivity requirements and power dissipation considerations also influence flexure and piezoresistor geometry. Shorter piezoresistors located near the root of the flexure will experience larger average bending moments and therefore yield higher force sensitivity. At the same time, for a given bridge excitation voltage, longer piezoresistors are required to limit Ohmic heat generation to acceptable levels.

Other features of the sensor design address the unique requirements of measuring living, and therefore unpredictable, organisms. The plasma-etched gaps between the suspended plate and flexure structure and the surrounding substrate are  $100\mu\text{m}$  wide, a dimension chosen to be large enough to allow for uniform through-wafer plasma etching and small enough

that the gaps would not distract a running insect. Because piezoresistors can be highly susceptible to ion contamination, it was necessary to isolate them from the environment and more specifically, from cockroach excretions. Toward this end, a  $2\mu\text{m}$  thick layer of silicon dioxide was deposited by LPCVD to act as an ionic barrier. This thick oxide also serves to protect the top surface of the devices, particularly the aluminum traces and interconnects, from damage as the cockroach runs over the silicon substrate.

To obtain usable force measurements from running cockroaches, sensors must be designed and installed in such a way that they will not interfere with the normal movement of the animal. Previous methods employed in the R. J. Full lab used a single sensor pad situated in the center of a 10cm wide walled running track. This pad was coupled mechanically to a large-scale force plate structure just below the running track [6]. In this configuration, many cockroach running trials were required to obtain even one good measurement as the insects would often miss the sensor pad completely. With this in mind, the present sensor design aims to address measurement efficiency issues by maximizing the number of experimental runs which will generate usable data. This is accomplished by arranging sensor elements in linear arrays as shown in Figure 5, thereby providing an effective sensing area of up to 8cm by 0.5cm for the larger twelve sensor element array. As the figure suggests, the maximum practical width of such an array is set by the size of a 10cm wafer. Arrays may be installed crosswise on the cockroach running track to maximize the likelihood that the insect will contact a pad as it traverses the track.

Figure 5 also indicates another important feature of the sensor arrays associated with the requirement of unimpeded insect motion. Light regions visible on the wafer are aluminum traces, all of which run from sensors in the middle of the wafer toward bond pads at its edges. By confining all wire bonds and off-wafer connections to the ends of each sensor array, the usable sensing area is maximized and the cockroach can move across the middle of the array without running afoul of bond wires or jumpers to off-chip electronics.



**Figure 6:** Sensor mounting. Test sensor elements are affixed in pairs to interchangeable printed circuit boards for wire-bonding.

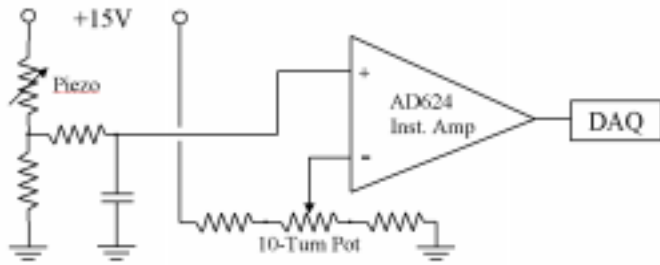


**Figure 7:** Full bridge balance, filter, and amplification circuit for one piezoresistor channel.

## EXPERIMENTAL SETUP

Individual test sensors were mounted and wire-bonded to off-the-shelf printed circuit boards as shown in Figure 6. Sections of double-sided adhesive tape act as spacers situated beneath the ends of each sensor die to provide the central shuttle plate with adequate clearance above the PCB. To provide added stiffness, epoxy resin was applied around the edge of the sensor die (not shown). Power supply and signal lines were connected to the PCB by a 34-pin ribbon cable and IDE connector. The entire assembly was fixed to an acrylic back-plate with a second ribbon cable attachment providing strain relief. The assembly was then fixed to the stage of a wafer probe-station microscope enclosed in an electromagnetically and acoustically insulated box. Room temperature was controlled at 20C for all piezoresistor measurements.

Eight channels of piezoresistor strain gauge data were sampled simultaneously using a National Instruments PCI-MIO-16XE-50 data acquisition board controlled with Labview on a PC. The average sampling rate of the DAQ system was 100 Hz. Figure 7 shows the configuration of the full bridge amplifier and signal conditioning circuit for a single piezoresistive strain gauge. The piezoresistor signal from the on-chip half-bridge was low-pass filtered with an 800Hz cutoff, then amplified by an Analog Devices 624 instrumentation amplifier with a fixed internal gain of 100.

Two classes of force measurements were conducted to evaluate sensor performance with respect to normal loads. Static load tests allowed the application of a known force to the sensor, while dynamic load tests used a piezoelectric actuator to apply controlled displacements to the sensor assembly.

For static load testing, small items of known mass were placed on the sensor pad and the resulting signals were averaged to determine the nominal sensitivity of the device with respect to normal forces. To obtain an easily variable and well-defined forces, small nylon nuts weighing from 0.26mN to 1.7mN were stacked on the sensor in different combinations. Nuts were weighed individually and in aggregate using a precision digital balance to establish the mass of the individual parts. Forces applied to the sensor using this method ranged from 0.26mN to around 9mN, a range of forces corresponding very well in scale to the ground reaction forces produced by running cockroaches.

Dynamic load testing was accomplished using a Melles Griot dual-axis piezoelectric actuator (Model 07TMF615) capable of producing repeatable displacements up to 45 $\mu$ m with nanometer resolution. The actuator provided fine positioning of a stylus which was used to load the sensor as shown in Figure 8. The tip shown above the sensor in this figure was ultimately replaced with a less compliant stylus to eliminate measurement errors associated with bending of the probe tip during loading. The actuator was controlled through Labview such that ramp displacement profiles could be applied to the sensor concurrently with eight-channel data acquisition. Normal displacements (and therefore forces) were applied at the center of the shuttle plate and at two eccentric locations along the horizontal and diagonal axes of symmetry respectively.

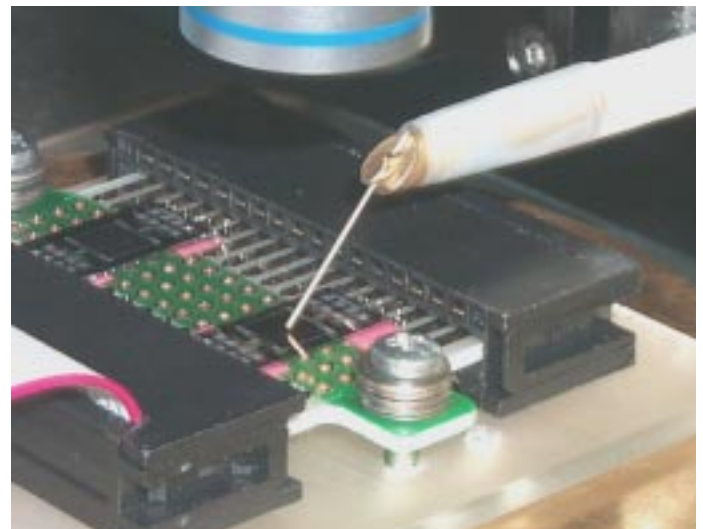


**Figure 8:** Experimental setup for dynamic loading. The piezoelectrically actuated probe tip is poised just above the sensor.

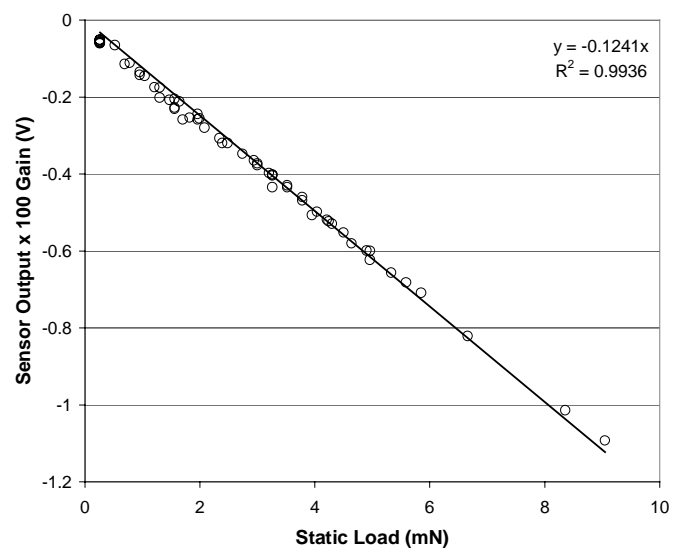


**Figure 9:** Force sensitivity to static normal loading. n=56

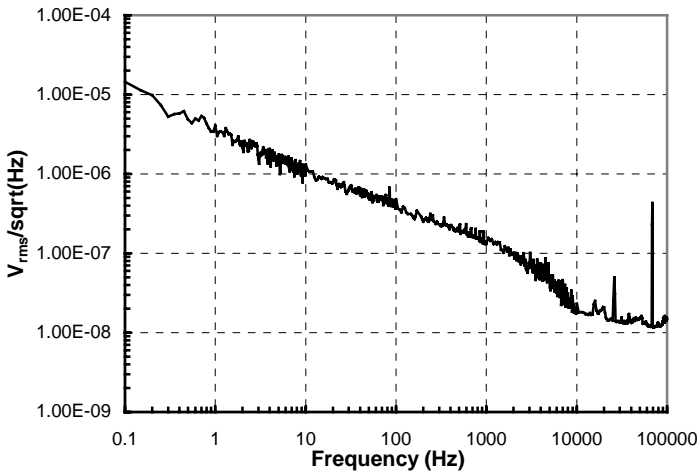


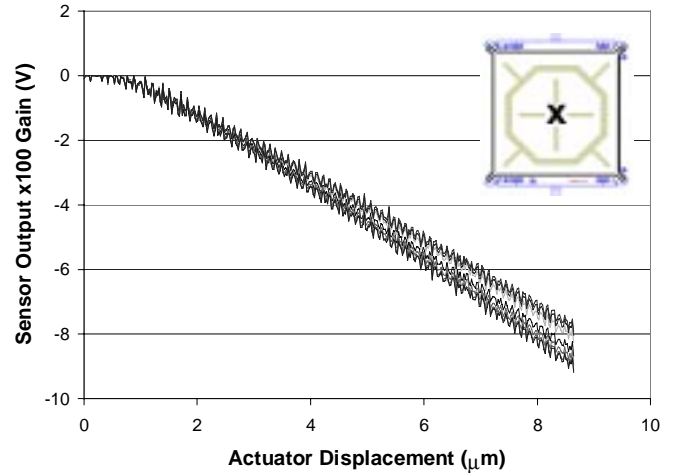
**Figure 10:** Noise Voltage spectrum for a typical mid-flexure piezoresistor.

## MEASUREMENTS AND RESULTS

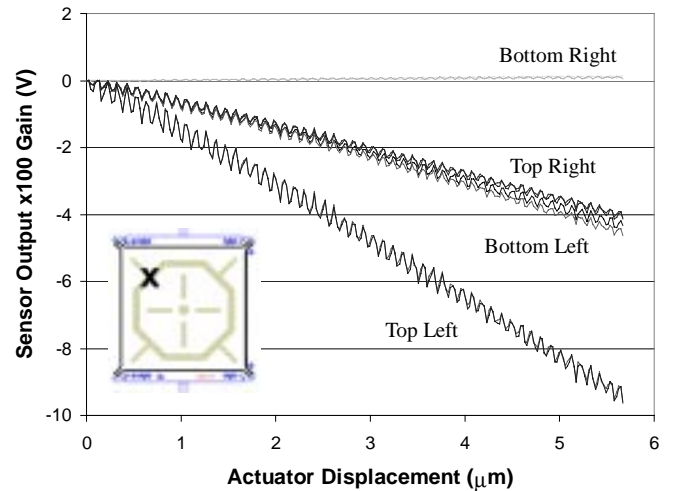
Figure 9 shows the results of the 54 static load experiments. For each load, signals from the four mid-flexure piezoresistors were averaged to obtain an equivalent output voltage with respect to centrally applied normal loading. As the plot shows, sensor response is quite linear and suggests an overall sensitivity to normal forces of approximately 1.2V/N without amplification. Variations in the data about the linear fit may be attributed primarily to uncertainty in the mass of the individual fasteners used to load the sensor.

Figure 10 shows a typical voltage noise spectrum for one of the mid-flexure piezoresistors. Both the piezoresistors and the passive legs of the sensor half-bridge have nominal values of 10kΩ with a bridge excitation of 15V. As indicated earlier, the half-bridge signal was low-pass filtered using a simple first-order filter with a cutoff at 800Hz. Below 800Hz, the plot shows a characteristic 1/f Hooge noise distribution [8]. The noise voltage associated with a typical piezoresistive measurement may be obtained by integrating the area under the noise density distribution across the measurement bandwidth of the device. Using a lower frequency bound of 1Hz and a nominal bandwidth of 800Hz, the voltage noise component of the signal will be approximately 8.7μV. For a normal force sensitivity of 1.2V/N as determined above, this suggests that the minimum normal force component resolvable by the sensor will be 7.3μN. This level of force resolution corresponds to measurements approximately three orders of magnitude smaller than the average normal forces typically exerted by running *Blaberus* cockroaches. Moreover, this result represents a nearly seventy-fold improvement over the resolution of the previous R.J. Full lab force plate.

While static loading tests produced quantitatively meaningful results, actuator displacement test results were less



**Figure 11:** Sensor response to centrally applied



**Figure 12:** Sensor response to corner load, diagonal symmetry.

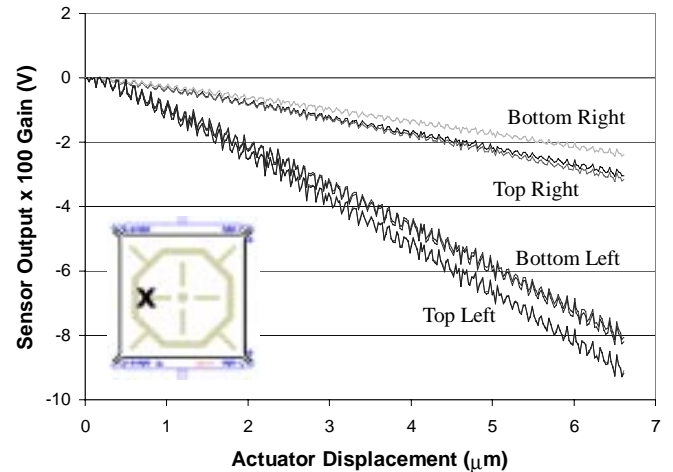


**Figure 13:** Sensor response to edge load, horizontal symmetry.

conclusive. Figures 11 through 13 show the sensor response to dynamic loads produced by the piezoelectric actuator. Based on the calculated stiffness of the sensor structure with respect to normal forces, there is a significant discrepancy between the force sensitivity indicated by static load measurements and that suggested by actuator displacement tests. Evidently, some component of the structure on which the sensor dice are mounted has a stiffness roughly 50 times softer than the  $0.426\text{N}/\mu\text{m}$  stiffness of the sensor in the normal direction. As a result, the sensor only experiences approximately 2% of the deflection suggested by these figures. Most likely this unwanted compliance arises from deflection of the PCB on which the sensor is mounted or the epoxy which supports the perimeter of the sensor die. Due to the stiffness of these sensor microstructures, future iterations on the experimental setup will require extraordinarily rigid fixturing to properly isolate the mechanical behavior of the sensor from that of its support.

Qualitatively, however, the signals shown in the actuator displacement plots are informative. The centrally applied load in Figure 11 produces strains in each of the flexures which are very nearly equal. Differences in slope among the eight signals suggest that the actuator stylus was not perfectly centered on the shuttle plate. Figure 12 shows the signals resulting from a pure normal force applied near one corner along a diagonal axis of symmetry. Figure 13 illustrates the response of the sensor to a force applied near one edge of the pad, lying on a horizontal axis of symmetry. In both cases, the figures demonstrate the expected symmetries and asymmetries in the piezoresistor strains associated with each loading case. Again, the actual displacement experienced by the sensor in these cases is roughly one fiftieth of the total actuator displacement, with the remainder of this displacement being accommodated by the compliance of the sensor mount rather than the sensor itself.

## CONCLUSIONS AND FUTURE WORK

Characterization of the performance of a new sensor intended for three-axis measurements of the small-scale forces produced by running cockroaches has begun. Un-amplified normal force sensitivity of  $1.2\text{V}/\text{N}$  has been demonstrated. Expected force resolution for an 800Hz measurement bandwidth is  $7.3\mu\text{N}$ , a improvement of nearly two orders of magnitude over the performance of the apparatus previously available for making such measurements.

Future work will focus on evaluating the sensitivity of these sensors to in-plane forces. Additional tests will determine whether output signals from the sensor can adequately describe tri-axial forces exerted on the sensor plate independent of the point of application of the force. Finally, sensors will be installed in the R.J. Full lab at Berkeley for live measurements on the cockroach, *Blaberus Discoidalis*.

## ACKNOWLEDGMENTS

Funding and support for this project were provided by Office of Naval Research Multi University Research Initiative

and a National Defense Science and Engineering Graduate Fellowship. Sensors were fabricated at the Stanford Nanofabrication Facility, part of the National Nanofabrication Users Network funded by the National Science Foundation under award number ECS9731294.

## REFERENCES

1. Bailey, S.A., Cham J.G., Cutkosky, M.R., Full, R.J. "Biomimetic Robotic Mechanisms via Shape Deposition Manufacturing." 9th International Symposium of Robotics Research, Snowbird, Utah, October 9-12, 1999, p. 321-327.
2. Buehler, M., Saranli, U., Papadopoulos, D., Koditschek, D.E. "Dynamic Locomotion with Four and Six-Legged Robots," Int. Symp. Adaptive Motion of Animals and Machines, Montreal, Aug 2000.
3. Nelson, G.M., and Quinn, R.D., "Posture Control of a Cockroach-like Robot," Proceedings of the 1998 IEEE International Conference on Robotics and Automation, Leuven, Belgium, 1998.
4. Full, R.J., Autumn, K., Chung, J.L., Ahn, A., "Rapid Negotiation of Rough Terrain by the Death-Head Cockroach." *American Zoologist*. 38:81A. 1998.
5. Kubrow, T.M., Full, R.J., "The Role of the Mechanical System in Control: A Hypothesis of Self-Stabilization in Hexapedal Runners." *Phil. Trans. Roy. Soc. London B*. 354, 849-862. 1999.
6. Full, R.J., Blickhan, R., Ting, L.H., "Leg Design in Hexapedal Runners." *J. Experimental Biology* 158, 369-390. 1991.
7. Kane, B.J. "A High-Resolution Traction Stress Sensor Array for Use in Robotic Tactile Determination." Stanford University Doctoral Dissertation, 1998. 369-391.
8. Harley, J.A., Kenny, T.W., "1/f Noise Considerations for the Design and Process Optimization of Piezoresistive Cantilevers." *Journal of Microelectromechanical Systems*, Vol. 9, No. 2, June 2000.